ORIGINAL ARTICLE

Study of the interactions of di- and tri-terpenes from Stillingia loranthacea with the enzyme NSP16-NSP10 of SARS-CoV-2

Estudo das interações de di- e tri-terpenos de Stillingia loranthacea com a enzima NSP16-NSP10 de SARS-CoV-2

João Batista de Andrade Neto[1,,4,5], Emanuelle Machado Marinho[2], Cecília Rocha da Silva[1,5], Lívia Gurgel do Amaral Valente Sá[1,4,5], Vitória Pessoa de Farias Cabral[1,5], Thiago Mesquita Cândido[1,5], Wildson Max Barbosa da Silva[4], Letícia Bernardo Barbosa[4], Bruno Coelho Cavalcanti[5], Pedro de Lima-Neto[2], Emmanuel Silva Marinho[3], Akenaton Onassis Cardoso Viana Gomes[4], Hélio Vitoriano Nobre Júnior[1,5]

1. School of Pharmacy, Laboratory for Bioprospection of Antimicrobial Molecules (LABIMAN), Federal University of Ceará, Fortaleza, CE, Brazil. 2. Department of Analytical Chemistry and Physical Chemistry, Group of Theoretical Chemistry (GQT), Science Center, Federal University of Ceará, Fortaleza-CE, 60.455-760, Brazil. 3. Department of Chemistry, Group for Theoretical Chemistry and Electrochemistry (GQTE), State University of Ceará, Limoeiro do Norte, Ceará, Brazil. 4. Christus University Center (UNICHRISTUS), Fortaleza, Ceará, Brazil. 5. Drug Research and Development Center, Federal University of Ceará, Fortaleza, CE, Brazil.

Abstract

Objective: This study aimed to evaluate the interactions of di- and tri-terpenes from Stillingia loranthacea with the enzyme NSP16-NSP10 of SARS-CoV-2, important for viral replication. **Methods**: The molecular docking technique was used to evaluate this interaction. **Results**: The analysis showed that the evaluated compounds obtained RMSD values of 0.888 to 1.944 Å and free energy of -6.1 to -9.4 kcal/mol, with the observation of hydrogen bonds, salt bridges, and pi-sulfur, pi-alkyl, and hydrophobic interactions. **Conclusion:** Thus, the results obtained show the potential of the compounds analyzed against the selected target. Since computer simulations are only an initial step in projects for the development of antiviral drugs, this study provides important data for future research.

Keywords: Terpenes; *Stillingia loranthacea;* SARS-Cov 2; Molecular docking.

Resumo

Objetivo: avaliar as interações de di- e tri-terpenos de Stillingia loranthacea com a enzima NSP16-NSP10 de SARS-CoV-2, importante para a replicação viral. **Métodos**: A técnica de docking molecular foi utilizada para avaliar essa interação. **Resultados:** A análise mostrou que os compostos avaliados obtiveram valores de RMSD de 0,888 a 1,944 Å e energia livre de -6,1 a -9,4 kcal/mol, observando-se ligações de hidrogênio, pontes salinas e pi-enxofre, pi-alquil, e interações hidrofóbicas. **Conclusão**: Assim, os resultados obtidos mostram o potencial dos compostos analisados frente ao alvo selecionado. Como as simulações computacionais são apenas um passo inicial nos projetos de desenvolvimento de medicamentos antivirais, este estudo fornece dados importantes para pesquisas futuras.

Palavras-chave: Terpenos; Stillingia loranthacea; SARS-Cov 2; Docagem molecular.

INTRODUCTION

In the 21st century, two types of human coronaviruses (HCoVs) with high pathogenic potential, the severe acute respiratory syndrome coronavirus (SARS-CoV) and the Middle Eastern respiratory syndrome coronavirus (MERS-CoV), emerged from their natural reservoirs, causing global epidemics with alarming morbidity and mortality[1]. In December 2019, another type of pathogenic HCoV was identified in Wuhan, China, the new 2019 coronavirus (2019-nCoV/SARS-CoV-2)[1–3], characterized as an enveloped beta-coronavirus with single-stranded, positive-sense RNA[3].

In this context, COVID-19, the disease caused by SARS-CoV-2, spread rapidly, infecting people in more than 200 countries/regions in only two months[4], evidencing its easy transmission between individuals. Scientists believe it is spread mainly by direct contact or by droplets spread by infected people when coughing or sneezing[5]. In March 2020, due to the occurrence of logarithmic expansion of cases globally, COVID-19 was declared a pandemic by the World Health Organization (WHO)[6]. In this context, it has had a significant impact on health systems around the world, in addition to devastating economic effects in the primary, secondary and tertiary sectors[7].

After the SARS-CoV outbreak in 2003, researchers began to explore different extracts, drugs, and antiviral molecules as potential agents against SARS-CoV[8]. In a review study[9], outlined the current status of natural compounds and/or their

Correspondence: João Batista de Andrade Neto. Universidade Federal do Ceara. Telephone number: # 55 85 3366 8274. E-mail: label_ufc@yahoo.com.br
Conflict of interest: The authors declare that there is no conflict of interest.
Received: 2022 Jan 5; Revised: 2022 May 20; 2022 May 25; Accepted: 2022 May 27

derivatives with potential action against different species of coronavirus (CoV), concluding that many natural products and medicinal plants offer preventive and therapeutic options against viral infections, and due to their natural origin, safety and low cost compared to synthetic drugs, they can be important complementary compounds to fight viruses, with strong potential for the development of medicines against CoV.

In this respect, terpenes and terpenoids are recognized diverse natural compounds that have a wide range of biological activities, as indicated by[10], including antitumor, anti-inflammatory, antioxidant, anticoagulant, sedative, and analgesic actions, thus having a broad spectrum of application in the pharmaceutical area[11, 12]. Studies have evaluated the antiviral activity of these substances present in extracts of species of the genus Stillingia (Euphorbiaceae)[13–15], plants found in South, Central, and North America, and on islands in the Pacific and Indian Oceans[14,16] performed in silico analysis of the main components of essential oils in a specific target of SARS-CoV-2, the protein spike. They concluded that the terpenes and phenylpropanoids identified in the study may play a vital role in inhibiting viral replication in the host system.

Molecular docking is an important method that can provide a forecast of the structure of ligand-receptor complexes[17]. It is one of the most frequently used methods for structure-based drug design due to the ability to accurately predict the conformation of ligands to the appropriate target[17, 18].

Thus, analysis of the interactions of certain molecules, such as terpenes, with potential for study against SARS-CoV-2[19] as important targets for viral replication, such as enzyme NSP16-NSP10 2'-O-methyltransferase from SARS-CoV-2, is important. According to [20], the stimulation of NSP16 2'-O-methyltransferase activity by NSP10 is a common mechanism of CoV, so inhibitors can be developed targeting this enzyme to control viral infection.

Given this, the objective of the study is to evaluate the interactions of di- and tri-terpenes from Stillingia loranthacea with the NSP16-NSP10 enzyme from SARS-CoV-2 using molecular docking.

MATERIALS AND METHODS

Enzyme Collection and Preparation

The structure of NSP16-NSP10 SARS-CoV-2 was obtained from the Protein Data Bank (https://www.rcsb.org/), identified in the repository as 1.98 Angstrom Resolution Crystal Structure of NSP16-NSP10 Heterodimer from SARS-CoV-2 in Complex with Sinefungin, PDB ID: 6WKQ. The resolution of 1.98 Å, was determined from X-ray diffraction (R-Value Free: 0.180, R-Value Work: 0.162). It is classified as a viral protein, organism [This is wrong grammatically, but I don't know how to correct it without risking a technical mistake.] Severe acute respiratory syndrome coronavirus 2 and expression system Escherichia coli BL21(DE3), Escherichia coli BL21. In the protein preparation process, all residues were removed and polar hydrogens were added[21, 22] producing favorable protonation states for molecular docking[23].

Obtaining and Preparing Ligands

All two-dimensional coordinates of the molecules were rendered according to[13] (Figure 1). The physicochemical properties were listed in Table 1. To obtain the three-dimensional structures in the most stable thermodynamic conformation, the ligands were optimized following an adaptation of the method proposed by[24,25]. In this step, semi-empirical quantum formalism was used, with the algorithms available in the code of the Molecular Orbital Package, Version 16.111W[26–28], which were used for optimization. The parametric method 7 (PM7)[29] was used, with Hartree-Fock approximation (HF) (self-consistent field method), for wave function, considering the molecule in the fundamental state and a vacuum[27].

Figure 1. Structural formula (A) and major microspecie at pH 7.3 (B) of di and triterpenes from the *Stillingia loranthacea*.

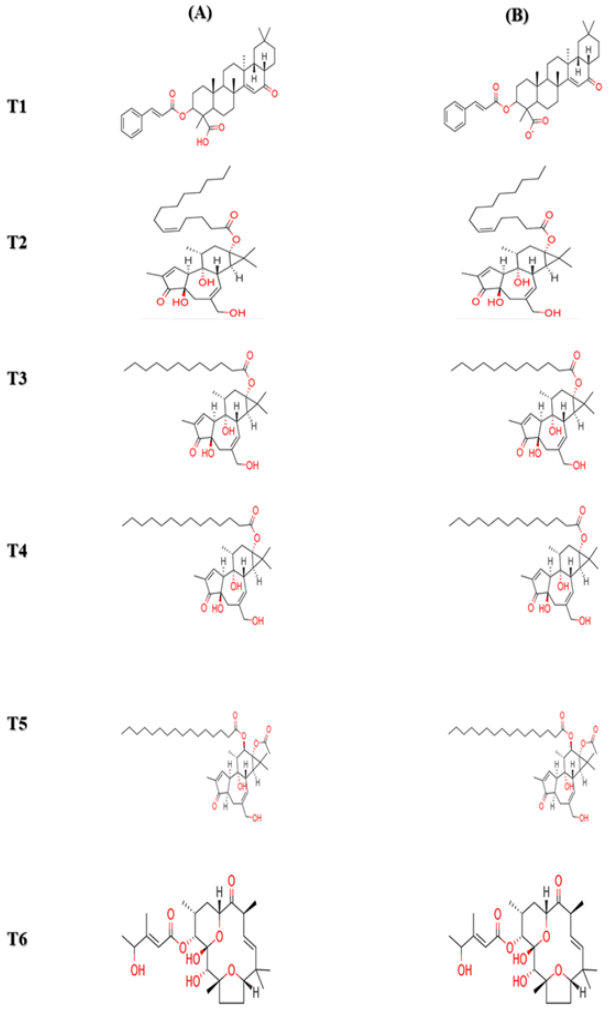

Table 1. Physical properties-clusters, lipophilicity and solubility of Di and triterpenes from the Stillingia loranthacea.

	Name	Formula	MW	pKa	H-bond		logP	TPSA	Solubility (mg/mL)
					D	A			
T1	(6aR,8aS,12aR,12bS,14bR)-4,6a,11,11,12b,14b-hexamethyl-8-oxo-3-{[(2E)-3-phenylprop-2-enoyl]oxy}-1,2,3,4,4a,5,6,6a,8,8a,9,10,11,12,12a,12b,13,14,14a,14b-icosahydropicene-4-carboxylic acid	C38H50O5	586.81	4.27	0	4	8.77	83.50	< 0.01
T2	(1R,2S,6R,10S,11R,13S,15R)-1,6-dihydroxy-8-(hydroxymethyl)-4,12,12,15-tetramethyl-5-oxotetracyclo[8.5.0.02,6.011,13]pentadeca-3,8-dien-13-yl (5Z)-tetradec-5-enoate	C34H52O6	556.78	12.57 14.01 15.19	3	5	5.92	104.06	< 0.01
T3	(1R,2S,6R,10S,11R,13S,15R)-1,6-dihydroxy-8-(hydroxymethyl)-4,12,12,15-tetramethyl-5-oxotetracyclo[8.5.0.02,6.011,13]pentadeca-3,8-dien-13-yl dodecanoate	C32H50O6	530.75	12.57 14.01 15.19	3	5	5.40	104.06	< 0.01
T4	(1R,2S,6R,10S,11R,13S,15R)-1,6-dihydroxy-8-(hydroxymethyl)-4,12,12,15-tetramethyl-5-oxotetracyclo[8.5.0.02,6.011,13]pentadeca-3,8-dien-13-yl tetradecanoate	C34H54O6	558.80	12.57	3	5	6.28	104.06	< 0.01
T5	(1R,2R,6R,10S,11R,13S,14R,15R)-13-(acetyloxy)-1-hydroxy-8-(hydroxymethyl)-4,12,12,15-tetramethyl-5-oxotetracyclo[8.5.0.02,6.011,13]pentadeca-3,8-dien-14-yl hexadecanoate	C38H60O7	628.89	13.92	2	5	7.44	110.13	< 0,01
T6	(1R,2S,3R,6S,8E,10S,12R,14R,15R)-1,2-dihydroxy-3,7,7,10,14-pentamethyl-11-oxo-16,17-dioxatricyclo[10.3.1.13,6]heptadec-8-en-15-yl (2E)-4-hydroxy-3-methylpent-2-enoate	C26H40O8	480.60	10.09 12.93 14.77 15.50	3	7	3.52	122.52	0.04

Molecular Docking

The simulations were configured to perform continuous calculations of cycles of 500 interactions with a convergence value on the order of 10-10 kcal mol^{-1} [30]. In this stage, the conformational stability of the compound is given by the total energy, which is the sum of the nuclear repulsive energies with the electronic energy. The fitting simulations between the selected inhibitors and the proteins were performed using the code AutoDock Vina (version 1.1.2), employing 3-way multithreading, the Lamarkian genetic algorithm[31], with the following docking parameters: m-pro(center_x = -26.734, center_y = 13.009, center_z = 56.185, size_x = 94, size_y = 112, size_z = 108, spacing = 0.642 and exhaustiveness = 8); NSP16-NSP10 (center_x = 78.486, center_y = -1.045, center_z = -9.341, size_x = 102, size_y = 126, size_z = 108, spacing = 0.764 and exhaustiveness = 8). As a standard procedure, 100 independent simulations were performed, obtaining 10 poses for each protein target. As selection criteria, simulations that presented poses with RMSD (root-mean-square deviation) values less than 2,000[32] and bond-free energy (ΔG) below -6.0 kcal/mol[33] were analyzed. To analyze the results, image plotting and generation of bi and tri-country maps the codes were used from the Discovery Studio Visualizer and UCSF Chimera[28,34].

RESULTS

Interactions of di- and tri-terpenes from Stillingia loranthacea with NSP16-NSP10 heterodimer

To better understand receptor-ligand interactions, the study of molecules through molecular docking has become increasingly relevant to predict modes of connection and elucidate experimental results [35]. With the molecular docking routines, we generated RMSD values [32] and connection-free energy [33] between the di- and tri-terpenes and the NSP16-NSP10 heterodimer, observing variations in the RMSD values from 0.888 to 1.944 Å and free binding energy ranging from -6.1 to -9.4 kcal/mol (Table 2). Analysis of the molecular docking simulations showed that all terpenes were bound in the same region as the inhibitor Sinefungin, more specifically in the heterodimer A chain NSP16-NSP10 heterodimer of SARS-CoV-2 (Figure 2).

By comparing the calculated distances between the inhibitors and the residues of the NSP16-NSP10 heterodimer binding site (Table 2), it was possible to observe that all the ligands were at a distance less than or equal to the inhibitor (Sinefungin) complexed in the NSP16-NSP10 heterodimer of SARS-CoV-2

(Figure 1). The interaction analysis showed that T1 exhibited eight interactions with the NSP16-NSP10 heterodimer, four of which are hydrophobic interactions, with Leu 7201C (3.50 Å; 3.55 Å), Tyr 7233C (3.36 Å) and Phe 7246C (3.85 Å); one hydrogen bond, with Asp 7176C (2.71 Å), classified as strong [36]; two of the PI-Alkyl type, with Leu 7201C and Cys 7216C; and one PI-sulfur interaction, with Met 7232C (Table 3).

Table 2. RMSD and affinity energy values calculated in molecular docking simulations by Di and triterpenes from Stillingia loranthaceain in NSP16-NSP10 Heterodimer from SARS-CoV-2 residues.

Inhibitor	Affinity (kcal/mol)	RMSD (Å)
T1	-9.4	1.523
T2	-6.7	1.163
T3	-7.0	1.270
T4	-6.9	0.888
T5	-6.1	1.333
T6	-7.7	1.944
Sinefugin	-6.6	1.362

Analyzing the receptor-ligand complex formed with T2 revealed eight ligand interactions with the enzyme's amino acid residues, three of which are of the hydrophobic type, with Lys 4346B (3.74 Å), Val 6902A (3.72 Å), and Val 7391C (3.77 Å); four hydrogen bonds, with Ser 6903A (2.46 Å), Ser 6907A (2.60 Å) and Thr 6908A (2.42 Å; 1.84 Å), all classified as strong [36]; and a salt bridge interaction, with Lys 4346B (3.61 Å) (Table 3).

The T3 inhibitor showed ten interactions with the NSP16-NSP10 heterodimer from SARS-CoV-2, three of the hydrophobic type, with Leu 6898A (3.71 Å), Ile 6910A (3.73 Å), and Val 7092A (3.44 Å); and seven hydrogen bonds, with Ile 6910A (2.44 Å), Ser 7090A (2.41 Å; 2.38 Å; 2.27 Å; 2.35 Å), Ser 7389C (2.01 Å), Ser 7389C (2.21 Å), all classified as strong [36] (Table 3).

Analyzing the receptor-ligand complex formed with T2 revealed eight ligand interactions with the enzyme's amino acid residues, three of which are of the hydrophobic type, with Lys 4346B (3.74 Å), Val 6902A (3.72 Å), and Val 7391C (3.77 Å); four hydrogen bonds, with Ser 6903A (2.46 Å), Ser 6907A (2.60 Å) and Thr 6908A (2.42 Å; 1.84 Å), all classified as strong [36]; and a salt bridge interaction, with Lys 4346B (3.61 Å) (Table 3).

Figure 2. The di- and tri-terpenes from Stillingia loranthacea binding the NSP16-NSP10 SARS COV 2 residues compared to sinefungin.

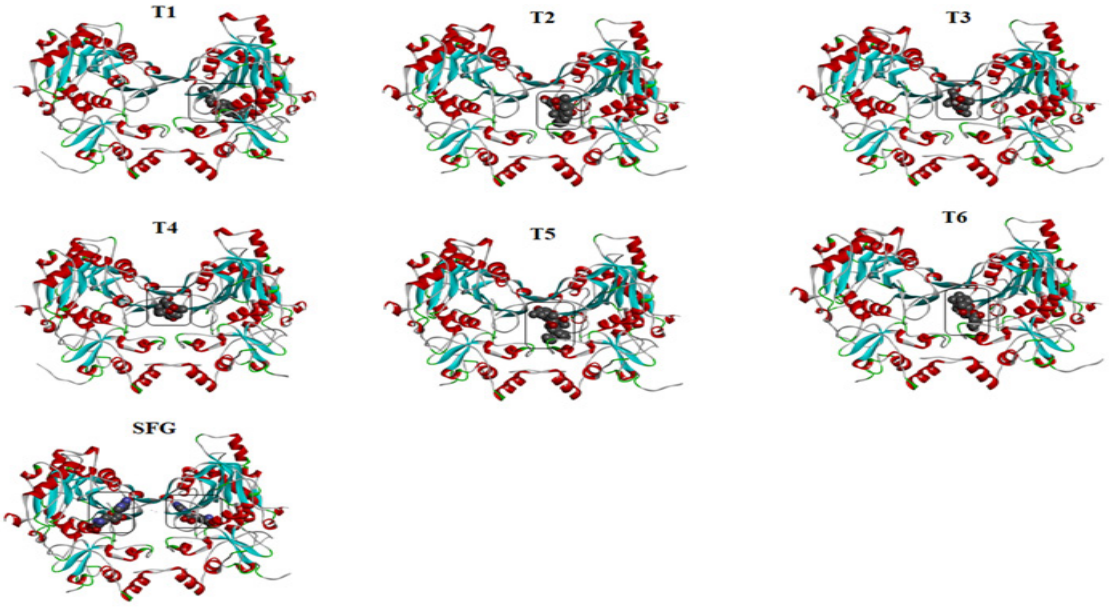

The T3 inhibitor showed ten interactions with the NSP16-NSP10 heterodimer from SARS-CoV-2, three of the hydrophobic type, with Leu 6898A (3.71 Å), Ile 6910A (3.73 Å), and Val 7092A (3.44 Å); and seven hydrogen bonds, with Ile 6910A (2.44 Å), Ser 7090A (2.41 Å; 2.38 Å; 2.27 Å; 2.35 Å), Ser 7389C (2.01 Å), Ser 7389C (2.21 Å), all classified as strong [36] (Table 3).

The analysis of the interactions with T4 showed that the molecular docking simulation of the inhibitor resulted in the formation of 12 interactions with the enzyme, five of which are hydrophobic, with the residues Ile 7213C (3.67 Å; 3.91 Å), Thr 7218C (3.86 Å), Val 7391C (3.36 Å) and Val 7391C (3.74 Å); and seven hydrogen bonds, with Ser 7090A (2.67 Å; 2.26 Å; 2.41 Å; 2.19 Å), Ile 7213C (2.44 Å; 2.84 Å) and Ser 7389C (2.16 Å), all classified as strong [36] (Table 3).

T5 showed seven interactions with the residues of the NSP16-NSP10 heterodimer, four hydrophobic, with Val 6902A (3.99 Å; 3.54 Å), Leu 6909A (3.85 Å), and Val 7391C (3.75 Å); and three hydrogen bonds, Thr 6908A (2.65 Å), Ile 6910A (2.16 Å) and Ser 7090A (2.10 Å), all classified as strong [36] (Table 3).

The T6 molecular docking routines showed the formation of nine interactions with the protein target, six hydrophobic, with Val 6902A (3.75 Å), Thr 6908A (3.95 Å), Leu 6909A (3.75 Å), Ile 6910A (3.94 Å), Ile 6910A (3.88 Å) and Val 7391C (3.93 Å); two hydrogen bonds, with Cys 4330B (1.98 Å) and Ile 6910A (3.34 Å), one classified as strong (Cys 4330B) and the other as medium (Ile 6910A) [36]; and one salt bridge interaction, with Lys 4346B (3.86 Å).

Table 3. Molecular interactions of the Di and triterpenes from Stillingia loranthaceain with the NSP16-NSP10 Heterodimer from SARS-CoV-2 residues.

			T1		
Hydrophobic Interactions	COVID-19 (NSP16-NSP10) residue a	Distance	-	Ligand Atom	Protein Atom
	Leu 7201C	3.50	-	34	5073
	Leu 7201C	3.55	-	37	5075
	Tyr 7233C	3.36	-	1	5364
	Phe 7246C	3.85	-	36	5500
Hydrogen Bonds	COVID-19 (NSP16-NSP10) residue a	Distance H-A	Classificationb	Donor Atom	Acceptor Atom
	Asp 7176C	2.71	Strong	4841 [Nam]	43 [O.co2]
PI-Alkyl	COVID-19 (NSP16-NSP10) residue a	-	-	-	-
	Leu 7201C	-	-	-	-
	Cys7216C	-	-	-	-
PI-Sulfur	COVID-19 (NSP16-NSP10) residue a	-	-	-	-
	Met 7232C	-	-	-	-
			T2		
Hydrophobic Interactions	COVID-19 (NSP16-NSP10) residue a	Distance	-	Ligand Atom	Protein Atom
	Lys 4346B	3.74		29	3691
	Val 6902A	3.72		23	1060
	Val 7391C	3.77		9	6965
Hydrogen Bonds	COVID-19 (NSP16-NSP10) residue a	Distance H-A	Classification	Donor Atom	Acceptor Atom
	Ser 6903A	2.46	Strong	1062 [Nam]	39 [O2]
	Ser 6907A	2.60	Strong	36 [O3]	1105 [O3]
	Thr 6908A	2.42	Strong	1116 [O3]	39 [O2]
	Thr 6908A	1.84	Strong	1110 [N3]	36 [O3]
Salt Bridges	COVID-19 (NSP16-NSP10) residue a	Distance	-	Ligand Group	Ligand Atoms
	Lys 4346B	3.61	-	Carboxylate	38, 39
			T3		
Hydrophobic Interactions	COVID-19 (NSP16-NSP10) residue a	Distance	-	Ligand Atom	Protein Atom
	Leu 6898A	3.71	-	27	1007
	Ile 6910A	3.73	-	19	1130
	Val 7092A	3.44	-	17	2959

Hydrogen Bonds	COVID-19 (NSP16-NSP10) residue a	Distance H-A	Classification	Donor Atom	Acceptor Atom
	Ile 6910A	2.44	Strong	1125 [Nam]	34 [O3]
	Ser 7090A	2.41	Strong	2942 [O3]	34 [O3]
	Ser 7090A	2.38	Strong	34 [O3]	2942 [O3]
	Ser 7090A	2.27	Strong	2931 [N3]	38 [O3]
	Ser 7090A	2.35	Strong	2932 [N3]	38 [O3]
	Ser 7389C	2.01	Strong	6936 [Nam]	38 [O3]
	Ser 7389C	2.21	Strong	38 [O3]	6939 [O2]
			T4		
Hydrophobic Interactions	COVID-19 (NSP16-NSP10) residue a	Distance	-	Ligand Atom	Protein Atom
	Ile 7213C	3.67	-	19	5182
	Ile 7213C	3.91	-	22	5183
	Thr 7218C	3.86	-	27	5218
	Val 7391C	3.36	-	17	6964
	Val 7391C	3.74	-	30	6965
Hydrogen Bonds	COVID-19 (NSP16-NSP10) residue a	Distance H-A	Classification	Donor Atom	Acceptor Atom
	Ser 7090A	2.67	Strong	2939 [O3]	40 [O3]
	Ser 7090A	2.26	Strong	2933 [N3]	40 [O3]
	Ser 7090A	2.41	Strong	2934 [N3]	40 [O3]
	Ser 7090A	2.19	Strong	40 [O3]	2940 [O2]
	Ile 7213C	2.44	Strong	5177 [Nam]	36 [O3]
	Ile 7213C	2.84	Strong	36 [O3]	5180 [O3]
	Ser 7389C	2.16	Strong	6938 [Nam]	40 [O3]
			T5		
Hydrophobic Interactions	COVID-19 (NSP16-NSP10) residue a	Distance	-	Ligand Atom	Protein Atom
	Val 6902A	3.99	-	26	1063
	Val 6902A	3.54	-	27	1064
	Leu 6909A	3.85	-	4	1129
	Val 7391C	3.75	-	3	6971
Hydrogen Bonds	COVID-19 (NSP16-NSP10) residue a	Distance H-A	Classification	Donor Atom	Acceptor Atom
	Thr 6908A	2.65	Strong	1114 [N3]	44 [O3]
	Ile 6910A	2.16	Strong	1131 [Nam]	43 [O3]
	Ser 7090A	2.10	Strong	2948 [O3]	43 [O3]
Salt Bridges	COVID-19 (NSP16-NSP10) residue a	Distance	-	Ligand Group	Ligand Atoms
	Lys 4346B	5.20	-	Carboxylate	44, 45

			T6		
Hydrophobic Interactions	COVID-19 (NSP16-NSP10) residue a	Distance	-	Ligand Atom	Protein Atom
	Val 6902A	3.75	-	24	1054
	Thr 6908A	3.95	-	16	1109
	Leu 6909A	3.75	-	18	1119
	Ile 6910A	3.94	-	16	1126
	Ile 6910A	3.88	-	7	1125
	Val 7391C	3.93	-	14	6958
Hydrogen Bonds	COVID-19 (NSP16-NSP10) residue a	Distance H-A	Classification	Donor Atom	Acceptor Atom
	Cys 4330B	1.98	Strong	32 [O3]	3527 [O2]
	Ile 6910A	3.34	Average	1121 [Nam]	29 [O2]
Salt Bridges	COVID-19 (NSP16-NSP10) residue a	Distance	-	Ligand Group	Ligand Atoms
	Lys 4346B	3.86	-	Carboxylate	30, 31

a. The crystal structure of COVID-19 main protease - PDB ID: 6LU7

b. Hydrogen bond classification: 2,5 Å <d <3,1 Å => Strong interaction; 3,1 Å <d <3,55 Å => Average interaction; d> 3,55 Å => Weak interaction

DISCUSSION

Potential therapies against CoV are classified because of their targets, which are related to the action of the main agent in the immune system, in host cells, or in the virus itself[37]. Thus, one of the ways to identify therapeutic options targeting the virus is through computational methods, which are carried out by[38] in the context of drug repositioning.

Terpenoids and terpenes produced by plants of the Euphorbiaceaea family have highly diverse structural compositions, one of the reasons that are a target in research for new drugs[39]. In this respect[40], evaluated the antiviral activity of diterpene compounds derived from the Euphorbiaceae family, which demonstrated the potent selective activity of these derivatives on the Chikungunya virus, HIV-1, and HIV-2, with EC50 = 0.76, IC50 = 0.34 and 0.043 µM, respectively. The study conducted by [13] also demonstrated the action of tri- and di-terpenoids derived from S. loranthacea against the Zika virus strain circulating in Brazil in an in vitro viral replication assay, further demonstrating its low cytotoxicity in epithelial cells.

The present study analyzed the interactions of di- and tri-terpenes from S. loranthacea with the NSS16-NSP10 enzyme from SARS-CoV-2, reported in the literature as a possible target for the development of antiviral drugs against CoV [20], by elucidating through in silico verification, the interactions of these substances with this target. A detailed understanding of the interactions between molecules and proteins can serve as the basis for more rational drug design, with the potential to reduce costs and time compared to traditional random screening protocols for the discovery of new drugs, besides being able to facilitate the development of more specific therapeutic agents[41].

Furthermore, the study of intermolecular interactions is of fundamental importance, since in biological systems, molecular recognition is based on specific stable interactions between molecules. In this context, one of the objectives of drug design is the identification of these interactions[42].

From the analysis of the results, all the compounds under study presented hydrogen bonds or hydrophobic interactions with the target in question. Hydrogen bonds are one of the most important types of interaction in molecular biology, by shaping three-dimensional structures of macromolecules and influencing their interactions with the surrounding environment and ligands[43]. Hydrophobic interactions have relevance in drug design considering the potential to increase the link affinity between drug and target interfaces[44]. According to the anti-SARS compound screening carried out by[45] through molecular docking, hydrogen bonds exercise, important collaboration is not said to respect the interactions between binder and receptor, so that in addition, as Hydrophobic Interactions we can make contributions to the total free energy of Gibbs induced by the binding, so that as Hydrogen Bonds can act as "âncora", determining the position of the binder in the binder bag, also facilitating Hydrophobic Interactions. In another study[46], cooperation between non-covalent bonds in a systematically varied series of ligands was assessed, and cooperation between hydrophobic interactions and hydrogen bonds was demonstrated, where they can reinforce each other. In addition to the mentioned interactions, it is important to note that compound T1 also showed PI-sulfur and PI-alkyl interactions. Sidechains containing sulfur can interact favorably with aromatic rings through PI interaction and can contribute to protein stability through non-covalent interactions[47].

Furthermore, Alkyl CH-PI interactions are known to be an important element in the molecular recognition between carbohydrates and proteins[48, 49].

Salt Bridges were also observed for compounds T2 and T6, which are configured in a non-covalent interaction between two ionized molecules, mixing two contributions, a hydrogen bond and an electrostatic bond, which in the case of a Salt Bridges formed in receptor-complex ligand, as with the compound T2, the proton can migrate a side chain of the carboxylic acid group to an amine fraction of a ligand (and vice versa) or the functional amino acid group[42]. In general, salt bridges directly contribute to binding and indirectly influence protein folding[50].

Regarding the free energy of binding, it varied from -6.1 to -9.4 kcal/mol for the interactions of the di- and tri-terpenes analyzed with the NSP16-NSP10 enzyme from SARS-CoV-2. These values are adequate according to the literature, which corresponds to - 6.0 kcal/mol or less[51].

CONCLUSION

Thus, the results of this study elucidate the interactions between the di- and tri-terpenes of S. loranthacea concerning the NSP16-NSP10 enzyme of SARS-CoV-2. The evaluation of the simulations using molecular docking demonstrated that the analyzed terpenes are bound in the same region as the inhibitor Sinefungin (NSP16-NSP10 heterodimer A chain) and that all ligands are present at a distance less than or equal to that of Sinefungin complexed in the enzyme in question. Regarding the interactions, hydrogen bonds, hydrophobic, Pi-sulfur, and Pi-alkyl interactions, and salt bridges were observed in the analyzed target. Furthermore, regarding the free energy of binding, the values found were adequate according to the standard considered in the literature. Thus, this study elucidates important molecular aspects regarding the analyzed compounds, providing important data for future studies.

ACKNOWLEDGMENTS

This study was supported by grants and fellowships from CNPq, CAPES, and FUNCAP. We declare no conflicts of interest concerning this article.

REFERENCES

1. Paules CI, Marston HD, Fauci AS. Coronavirus Infections—More Than Just the Common Cold. Jama. 2020 Feb; 323(8): 707–708. doi: https://doi.org/10.1001/jama.2020.0757.

2. Chen N, Zhou M, Dong X, Qu J, Gong F, Han Y, et al (2020) Epidemiological and clinical characteristics of 99 cases of 2019 novel coronavirus pneumonia in Wuhan, China: a descriptive study. Lancet. 2020 Jan; 395(10223): 507–513. doi: https://doi.org/10.1016/S0140-6736(20)30211-7.

3. Li G, De Clercq E. Therapeutic options for the 2019 novel coronavirus (2019-nCoV). Nat Rev Drug Discov. 2020 Mar; 19(3):149–150. doi: https://doi.org/10.1038/d41573-020-00016-0.

4. Ahmad T, Harroon, Baig M, Hui J. Coronavirus Disease 2019 (COVID-19) Pandemic and economic impact. Pak J Med Sci. 2020 May; 36 (COVID19-S4): S73–S78. doi: https://doi.org/10.12669/pjms.36.COVID19-S4.2638.

5. Rothan HA, Byrareddy SN. The epidemiology and pathogenesis of coronavirus disease (COVID-19) outbreak. J Autoimmun. 2020 May; 109: 102433. doi: https://doi.org/10.1016/j.jaut.2020.102433.

6. Kakodkar P, Kaka N, Baig M. A Comprehensive Literature Review on the Clinical Presentation, and Management of the Pandemic Coronavirus Disease 2019 (COVID-19). Cureus. 2020 Apr; 12(4): e7560. doi: https://doi.org/10.7759/cureus.7560.

7. Nicola M, Alsafi Z, Sohrabi C, Al-Jabir A, Iosifidis C, Agha M, et al. The socio-economic implications of the coronavirus pandemic (COVID-19): A review. Int J Surg.2020 Jun; 78: 185–193. doi: https://doi.org/10.1016/j.ijsu.2020.04.018.

8. Boukhatem MN, Setzer WN. Aromatic herbs, medicinal plant-derived essential oils, and phytochemical extracts as potential therapies for coronaviruses: Future perspectives. Plants; 9(6): 9:1–23. doi: https://doi.org/10.3390/PLANTS9060800.

9. Islam MT, Sarkar C, El-Kersh DM, Jamaddar S, Uddin SJ, Shipi JA, et al. Natural products and their derivatives against coronavirus: A review of the non-clinical and pre-clinical data. Phyther Res. 2020 Oct; 34(10): 2471-2492. doi: https://doi.org/10.1002/ptr.6700.

10. Zhao DD, Jiang LL, Li HY, Yan P-F, Zhan Y-L. Chemical components and pharmacological activities of terpene natural products from the genus paeonia. Molecules. 2016 Oct; 21(10). doi: https://doi.org/10.3390/molecules21101362.

11. Ludwiczuk, A., Skalicka-Woźniak, K., & Georgiev, M. I. (2017). Terpenoids: Pharmacognosy. doi: https://doi.org/10.1016/B978-0-12-802104-0.00011-1.

12. Tetali SD. Terpenes and isoprenoids: a wealth of compounds for global use. Planta. 2019 Jan; 249(1): 1–8. doi: https://doi.org/10.1007/s00425-018-3056-x.

13. Abreu LS, Nascimento YM, Costa RS, Guedes MLS, Souza BNRF, Pena LJ, et al. Tri- and Diterpenoids from Stillingia loranthacea as Inhibitors of Zika Virus Replication. J Nat Prod. 2019; 82: 2721–2730. doi: https://doi.org/10.1021/acs.jnatprod.9b00251.

14. Olivon F, Palenzuela H, Girard-Valenciennes E, Neyts J, Pannecouque C, Pannecouque C, et al. Antiviral Activity of Flexibilane and Tigliane Diterpenoids from Stillingia lineata. J Nat Prod. 2015 May; 78(5): 1119–1128. doi: https://doi.org/10.1021/acs.jnatprod.5b00116.

15. Techer S, Girard-Valenciennes E, Retailleau P, Neytis J, Guéritte F, Leyssen P, et al. Tonantzitlolones from Stillingia lineata ssp. lineata as potential inhibitors of chikungunya virus. Phytochem Lett. 2015 Jun; 12: 313–319. doi: https://doi.org/10.1016/j.phytol.2015.04.023.

16. Kulkarni SA, Nagarajan SK, Ramesh V, Palaniyandi V, Selvam SP, Madhavan T. Computational evaluation of major components from plant essential oils as potent inhibitors of SARS-CoV-2 spike protein. J Mol Struct. 2020 Dec; 1221: 128823. doi: https://doi.org/10.1016/j.molstruc.2020.128823.

17. Meng X-Y, Zhang H-X, Mezei M, Cui M. Molecular Docking: A Powerful Approach for Structure-Based Drug Discovery. Curr Comput Aided-Drug Des. 2011 Jun; 7(2): 146–157. doi: https://doi.org/10.2174/157340911795677602.

18. Ferreira LG, Santos RN, Oliva G, Andricopulo AD. Molecular docking and

structure-based drug design strategies. Molecules. 2015 Jul; 20(7): 13384–13421. doi: https://doi.org/10.3390/molecules200713384.

19. Boukhatem MN. Effective Antiviral Activity of Essential Oils and their Characteristics Terpenes against Coronaviruses: An Update. J Pharmacol Clin Toxicol. 2020; 8(1): 1138.

20. Wang Y, Sun Y, Wu A, Xu S, Pan R, Zeng C, et al. Coronavirus nsp10/nsp16 Methyltransferase Can Be Targeted by nsp10-Derived Peptide In Vitro and In Vivo To Reduce Replication and Pathogenesis. J Virol. 2015 Aug; 89(16): 8416–8427. doi: https://doi.org/10.1128/jvi.00948-15.

21. Guerra TM. Estudos de Docking Molecular de Derivados da Tiazolidina Como Potenciais Inibidores da Enzima Cruzaína de Trypanosoma cruz [TCC]. Serra Talhada (PE): Universidade Federal Rural de Pernambuco; 2019.

22. Lucio FNM, Silva JE, Marinho EM, Mendes FRS. Methylcytisine Alcaloid Potentially Active Against Dengue Virus: A Molecular Docking Study And Electronic Structural Characterization. 2020 Feb. doi: https://doi.org/10.5281/zenodo.3633270.

23. Milite C, Amendola G, Nocentini A, Bua S, Cipriano A, Barresi E, et al. Novel 2-substituted-benzimidazole-6-sulfonamides as carbonic anhydrase inhibitors: synthesis, biological evaluation against isoforms I, II, IX and XII and molecular docking studies. J Enzyme Inhib Med Chem. 2019 Dec; 34(1): 1697–1710. doi: https://doi.org/10.1080/14756366.2019.1666836.

24. Dewar MJS, Zoebisch EG, Healy EF, Stewart JJP. Development and use of quantum mechanical molecular models. 76. AM1: a new general purpose quantum mechanical molecular model. J Am Chem Soc. 1985; 107(13): 3902-3909. doi: https://doi.org/10.1021/ja00299a024.

25. Bani-Yaseen AD. Computational molecular perspectives on the interaction of propranolol with β-cyclodextrin in solution: Towards the drug-receptor mechanism of interaction. J Mol Liq. 2017 Feb; 227: 280–290. doi: https://doi.org/10.1016/j.molliq.2016.12.023.

26. Stewart JJP. Optimization of parameters for semiempirical methods V: Modification of NDDO approximations and application to 70 elements. J Mol Model. 2007 Dec; 13(12): 1173-213. doi: https://doi.org/10.1007/s00894-007-0233-4.

27. Stewart JJP. Optimization of parameters for semiempirical methods VI: More modifications to the NDDO approximations and re-optimization of parameters. J Mol Model. 2013 Jan; 19(1): 1–32. doi: 10.1007/s00894-012-1667-x.

28. Marinho EM, Batista de Andrade Neto J, Silva J, Rocha da Silva C, Cavalcanti BC, Marinho ES, Nobre Júnior HV. Virtual screening based on molecular docking of possible inhibitors of Covid-19 main protease. Microb Pathog. 2020 Nov;148:104365. doi: 10.1016/j.micpath.2020.104365. Epub 2020 Jun 30. PMID: 32619669; PMCID: PMC7834391.

29. Dral PO, Wu X, Spörkel L, Koslowski A, Weber W, Steiger R, et al. Semiempirical quantum-chemical orthogonalization-corrected methods: theory, implementation, and parameters. J Chem Theory Comput. 2016 Mar; 12(3): 1082–1096. doi: 10.1021/acs.jctc.5b01046.

30. Arroio A, Honório KM, Silva ABF. Propriedades químico-quânticas empregadas em estudos das relações estrutura-atividade. Quim Nova. 33(3): 694–699. doi: https://doi.org/10.1590/S0100-40422010000300037.

31. Trott O, Olson AJ. AutoDock Vina: Improving the Speed and Accuracy of Docking with a New Scoring Function, Efficient Optimization and Multithreading. J Compit Chem. 2010 Jan; 31(2): 455-461. doi: https://doi.org/10.1002/jcc.

32. Yusuf D, Davis AM, Kleywegt GJ, Schmitt S. An Alternative Method for the Evaluation of Docking Performance : RSR vs RMSD. 2008; 48(7): 1411–1422. doi: https://doi.org/10.1021/ci800084x.

33. Shityakov S, Förster C. In silico predictive model to determine vector-mediated transport properties for the blood-brain barrier choline transporter. Adv Appl Bioinforma Chem. Adv Appl Bioinform Chem. 2014 Sep; 7: 23–36. doi; https://doi.org/10.2147/AABC.S63749.

34. Pettersen EF, Goddard TD, Huang CC, Couch GS, Greenblatt DM, Meng EC, et al. UCSF Chimera — A Visualization System for Exploratory Research and Analysis. J Comput Chem. 2004 Oct; 25(13): 1605-12. doi: https://doi.org/10.1002/jcc.20084.

35. Freitas TC, Oliveira RJ, Mendonça RJ, Candido PA. Identification of bioactive compounds and analysis of inhibitory potential of the digestive enzymes from syzygium sp. Extracts. J Chem. 2019 Feb; 47: 1-10. doi: https://doi.org/10.1155/2019/3410953.

36. Jonathan W. Steed JLA. Supramolecular Chemistry. 2nd ed. Wiley; 2009.

37. Gyebi GA, Ogunro OB, Adegunloye AP, Ogunyemi OM, Afolabi SO. Potential inhibitors of coronavirus 3-chymotrypsin-like protease (3CLpro): an in silico screening of alkaloids and terpenoids from African medicinal plants. J Biomol Struct Dyn. 2021 Jun; 39(9): 3396-3408. doi: https://doi.org/10.1080/07391102.2020.1764868.

38. Mahdian S, Ebrahim-Habibi A, Zarrabi M (2020) Drug repurposing using computational methods to identify therapeutic options for COVID-19. J Diabetes Metab Disord. 2020 May; 19(2): 691-699. doi: https://doi.org/10.1007/s40200-020-00546-9.

39. Remy S, Litaudon M. Macrocyclic diterpenoids from Euphorbiaceae as a source of potent and selective inhibitors of chikungunya virus replication. Molecules. 2019 Jun; 24(12): 2336. doi: https://doi.org/10.3390/molecules24122336.

40. Nothias-Scaglia LF, Retailleau P, Paolini J, Pannecouque C, Neyts J, Dumontet V, et al. Jatrophane diterpenes as inhibitors of chikungunya virus replication: Structure-activity relationship and discovery of a potent lead. J Nat Prod. 2014 Jun; 77(6): 1505–1512. doi: https://doi.org/10.1021/np500271u.

41. Lybrand TP. Ligand-protein docking and rational drug design. Curr Opin Struct Biol. 1995 Apr; 5(2): 224–228. doi: https://doi.org/10.1016/0959-440X(95)80080-8.

42. Kurczab R, Śliwa P, Rataj K, Kafel R, Bojarski AJ. Salt Bridge in Ligand-Protein Complexes - Systematic Theoretical and Statistical Investigations. J Chem Inf Model. 2018 Nov; 58(11): 2224–2238. doi: https://doi.org/10.1021/acs.jcim.8b00266.

43. Wahl MC, Sundaralingam M. C-H... hydrogen bonding in biology. Trends Biochem Sci. 1997 Mar; 22(3): 97–102. doi: https://doi.org/10.1016/S0968-0004(97)01004-9.

44. Patil R, Das S, Stanley A, Yadav L, Sudhakar A, Varma AK, et al. Optimized hydrophobic interactions and hydrogen bonding at the target-ligand interface leads the pathways of Drug-Designing. PLoS One. 2010 Aug; 5(8): e12029. doi: https://doi.org/10.1371/journal.pone.0012029.

45. Wei DQ, Zhang R, Du QS, Gao WN, Li Y, Gao H, et al. Anti-SARS drug screening by molecular docking. Amino Acids. 2006 Jul; 31(1): 73–80. doi: https://doi.org/10.1007/s00726-006-0361-7.

46. Muley L, Baum B, Smolinski M, Freindorf M, Heine A, Klebe G, et al. Enhancement of hydrophobic interactions and hydrogen bond strength by cooperativity: Synthesis, modeling, and molecular dynamics simulations of a congeneric series of thrombin inhibitors. J Med Chem. Mar 2010; 53: 2126–2135. doi: https://doi.org/10.1021/jm9016416.

47. Yan S, Lee S-J, Kang S-W, Choi K-H, Rhee S-K, Lee J-Y. Attractive sulfur⍰π interaction between fluorinated dimethyl sulfur (FDMS) and benzene. Bull Korean Chem Soc. 2007; 28(6): 959–964. doi: https://doi.org/10.5012/bkcs.2007.28.6.959.

48. Neel AJ, Hilton MJ, Sigman MS, Toste FD. Exploiting non-covalent π interactions for catalyst design. Nature. 2007 Mar; 543: 637–646. doi: https://

doi.org/10.1038/nature21701.

49. Asensio JL, Ardá A, Cañada FJ, Jiménez-Barbero J. Carbohydrate-aromatic interactions. Acc Chem Res. 2013; 46(4): 946–954. doi: https://doi.org/10.1021/ar300024d.

50. Zhou P, Huang J, Tian F. Specific Noncovalent Interactions at Protein-Ligand Interface: Implications for Rational Drug Design. Curr Med Chem. 2012; 19(2): 226–238. doi: https://doi.org/10.2174/092986712803414150.

51. Marinho EM, Andrade JB Neto, Silva J, Silva CR, Cavalcanti BC, Marinho ES, et al. Virtual screening based on molecular docking of possible inhibitors of Covid-19 main protease. Microb Pathog. 2020 Nov; 148: 104365. doi: https://doi.org/10.1016/j.micpath.2020.104365.

Como citar este artigo/ How to cite this article:
Andrade JB Neto, Marinho EM, Silva CR, Sá LGAV, Cabral VPF, Cândido TM et al. Study of the interactions of di- and tri-terpenes from Stillingia loranthacea with the enzyme NSP16-NSP10 of SARS-CoV-2. J Health Biol Sci. 2022; 10(1):1-10.